Aeolian Research 38 (2019) 39–47

Contents lists available at ScienceDirect

Aeolian Research

journal homepage: www.elsevier.com/locate/aeolia

Isotope fingerprinting reveals western North American sources of modern dust in the Uinta Mountains, Utah, USA

Jeffrey S. Munroe[a,*], Emmet D. Norris[a], Gregory T. Carling[b], Brian L. Beard[c], Aaron M. Satkoski[c,1], Lianwen Liu[d]

[a] Geology Department, Middlebury College, Middlebury, VT 05753, United States
[b] Department of Geological Sciences, Brigham Young University, Provo, UT 84602, United States
[c] Department of Geoscience, University of Wisconsin-Madison, Madison, WI 53706, United States
[d] Department of Earth Sciences, Nanjing University, Nanjing 210046, China

ARTICLE INFO

Keywords:
Dust
Rocky Mountains
Isotopic fingerprint
$^{87}Sr/^{86}Sr$
ε_{Nd}

ABSTRACT

The deposition of aeolian dust has profound effects on biogeochemical cycling, soil development, and hydrology in alpine ecosystems. In the western United States, it has been proposed that much of the dust reaching the Rocky Mountains is derived from arid regions located to the west-southwest. Because these areas are vulnerable to drought-related changes in vegetation, grazing impacts, mining, off-road vehicle travel, urban development, and other factors that affect the availability of fine-grained sediment for wind deflation, it is imperative that source areas for this dust be better constrained to guide future management decisions. Here we collect modern dust in the Uinta Mountains (Utah) and compare its $^{87}Sr/^{86}Sr$ and $^{143}Nd/^{144}Nd$ "fingerprint" with surficial sediments in possible source areas. Our results confirm that this dust is exotic to the Uinta Mountains, and demonstrate its similarity to numerous dune fields in western Utah, as well as surficial sediments in parts of the Colorado Plateau, southern Basin and Range, and the Mojave Desert. The seasonal sampling we employed also reveals that considerable dust is deposited during the shorter alpine summer. Recognition that specific areas in the southwestern US are sources of dust to the Rocky Mountains, particularly during summer months, should be considered in future land management planning.

1. Introduction

Recent research has illuminated the tremendous significance of mineral dust deposition in high elevation environments of the Rocky Mountains in the western United States. The deposition of dust influences soil development (Lawrence et al., 2013, 2011), adds trace metals to mountain snowpack and watersheds (Carling et al., 2012; Dastrup et al., 2018; Reynolds et al., 2010), and changes the nutrient status and sedimentation rate in high elevation lakes (Ballantyne et al., 2011; Brahney et al., 2014; Neff et al., 2008; Psenner, 1999; Zhang et al., 2018). Dust also decreases snowpack albedo (Painter et al., 2012; Reynolds et al., 2013; Skiles et al., 2012; Skiles and Painter, 2017), which shortens the duration of winter snow cover (Painter et al., 2007). This change steepens the rising limb of downstream hydrographs (Painter et al., 2018, 2010), and advances the timing of peak streamflow (Painter et al., 2010).

Several types of observations suggest that arid landscapes in the southwestern US are primary sources for dust arriving in the Rocky Mountains. These include the proximity of these areas to the Rocky Mountains (Lawrence et al., 2010); the grain size distribution of the dust, which is consistent with transport on the order of 100's of kilometers (Lawrence and Neff, 2009; Mahowald et al., 2005; Neff et al., 2008); generally south to north winds associated with dust storms (Hahnenberger and Nicoll, 2012); ground-based measurements of total suspended particulate (Reynolds et al., 2016); back-trajectory modeling (Dastrup et al., 2018; Hahnenberger and Nicoll, 2012; Reynolds et al., 2016); and dust plumes tracked on satellite imagery (Hahnenberger and Nicoll, 2014; Painter et al., 2007; Prospero et al., 2002). However, this theory has not been tested with an extensive geochemical comparison between modern dust in the Rocky Mountains and surficial sediments in potential source areas.

Radiogenic isotopes can be used as fingerprints to identify the provenance of aeolian sediments (Grousset and Biscaye, 2005; Marx et al., 2018). This approach has been extensively employed in studies of

* Corresponding author.
E-mail address: jmunroe@middlebury.edu (J.S. Munroe).
[1] Current affiliation: Jackson School of Geosciences, University of Texas-Austin, Austin, TX 78712, United States.

https://doi.org/10.1016/j.aeolia.2019.03.005
Received 4 December 2018; Received in revised form 20 March 2019; Accepted 21 March 2019

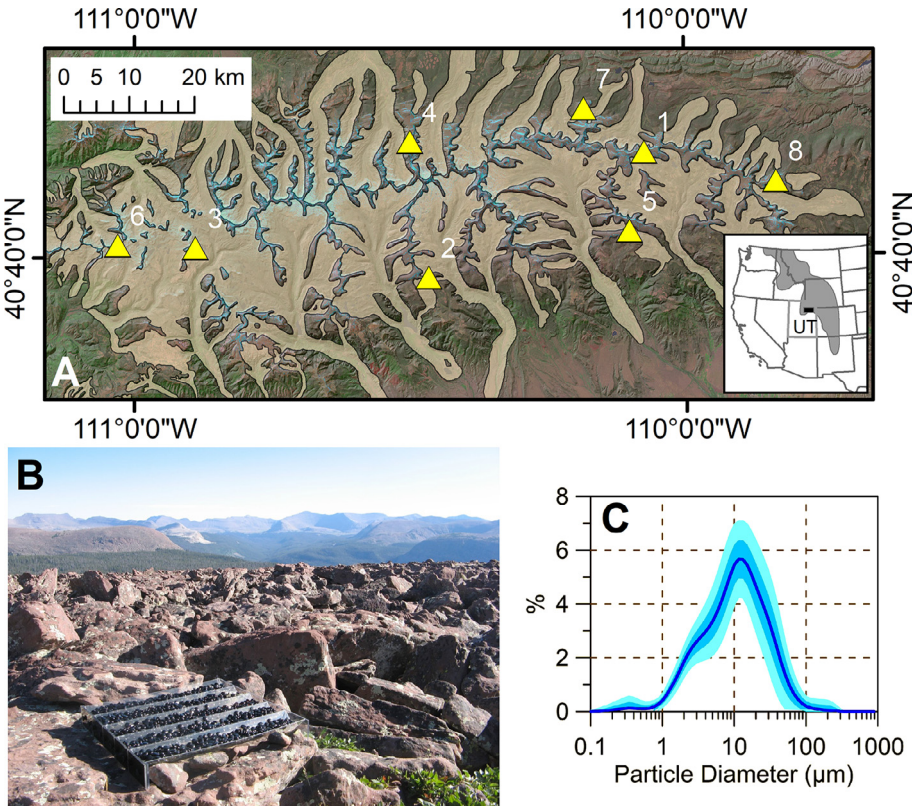

Fig. 1. Overview of the dust collector network in the Uinta Mountains, with the average grain size of collected dust. (A) Locations of the 8 passive dust collectors (yellow triangles) in the Uinta Mountains. The active sampler is co-located with the Dust-1 passive collector. Shapes denote the extent of glacier ice at the Last Glacial Maximum (Munroe and Laabs, 2009). Inset shows the location of the Uinta Mountains in the state of Utah (UT) in the western United States and the general area of the Rocky Mountain system (gray). (B) Representative photograph of a passive dust collector (Dust-2). (C) Average grain size distribution (dark blue) of Uinta dust samples (n = 44) collected between 2011 and 2017. Lighter shades of blue represent 1-σ and 2-σ ranges.

Chinese loess (Chen et al., 2007; Wang et al., 2007), trans-Atlantic transport of dust from North Africa to the Amazon and Caribbean (Kumar et al., 2014; Pourmand et al., 2014; Zhao et al., 2018), and to ascertain the sources of dust in Greenland ice cores (Bory et al., 2003; Lupker et al., 2010; Újvári et al., 2015). In the Rocky Mountains, radiogenic isotopes have been used on a limited basis to demonstrate dissimilarity between deposited dust and underlying bedrock (Aarons et al., 2016; Goldstein et al., 2008; Neff et al., 2008), but dust has not previously been compared with potential source areas.

Here we employ the radiogenic isotope ratios $^{87}Sr/^{86}Sr$ and $^{143}Nd/^{144}Nd$ to directly test the theory that dust deposited at high-elevations in the Rocky Mountains is sourced from the southwestern US.

2. Setting and methods

The study area for this work is the Uinta Mountains in northeastern Utah (Fig. 1). The Uinta Mountains (hereafter, the "Uintas") are a significant mountain range within the Rocky Mountain system, with maximum elevations > 4 km above sea level. Bedrock of the Uintas is a several-km thick sequence of siliciclastic metasedimentary rocks, ranging from shale to conglomerate, that accumulated in a Precambrian aulocogen and was uplifted during the Laramide Orogeny (Bradley, 1995; Dehler et al., 2007; Sears et al., 1982). No glaciers are present in the Uintas today, but repeated Quaternary glaciations exploited pre-existing stream drainages, producing a series of extensive U-shaped valleys (Laabs and Carson, 2005; Munroe, 2005). These valley glaciers only locally overtopped the interfluves (Atwood, 1909; Munroe and Laabs, 2009), and as a result, much of the Uinta ridgecrest is a winding, unglaciated landscape dominated by periglacial processes (Munroe, 2006). Previous work has demonstrated that soils in this alpine zone have been strongly influenced by dust deposition (Bockheim et al., 2000; Bockheim and Koerner, 1997; Munroe, 2007; Munroe et al., 2015).

Dust samples (n = 28) were collected in the Uintas during both winter (October–June) and summer (June–October) seasons using a network of 8 passive collectors (Munroe, 2014). These collectors are based on the classic marble dust trap (Goossens and Offer, 2000; Reheis and Kihl, 1995; Sow et al., 2006) and have been modified to work in a relatively high precipitation environment (Figs. 1B and A-1). The eight collectors were deployed at high elevations (> 3350 m asl) in a pattern intended to encompass the full extent of the Uintas (Fig. 1A). A specially designed active collector that captures discrete samples delivered by north and south winds was also deployed at the location of one of the passive dust samplers (Dust-1) where the wind regime is strongly bimodal (Figs. A-2 and A-3). This device uses solar-powered fans to pull air through a tube filled with glass marbles. A wind vane connected to a pair of microswitches turns the appropriate fan on and off when the wind is coming from either the NW or the S at velocities in excess of ~5 m/s. Details of the passive and active dust samplers can be found in the Appendix.

In the laboratory, dust washed from the collectors with distilled water was concentrated by centrifugation, treated with 35% H_2O_2 (~5–10 days) to remove organic matter, and sieved to 63 μm to remove sand-sized material that is presumably locally sourced. The grain size distribution of these samples was then analyzed with laser scattering in a Horiba LA950-v2. This instrument has an effective range from 10 nm to 3 mm, and a refractive index of 1.54 with an imaginary component of 0.1i is used in the calculating the grain size distribution on a volume basis. The remaining fraction of each sample was oven dried and ground before further analysis.

All dust samples were analyzed for Sr and Nd isotope ratios at the University of Wisconsin-Madison. Four representative samples of siliciclastic bedrock from the sites of collectors 1, 2, 4, and 8 were also analyzed in parallel with the dust samples. Samples were dissolved in concentrated HF and HNO_3, followed by HCl. Cation exchange columns were used to isolate Sr and rare earth elements. Aliquots were then analyzed using thermal ionization mass spectrometry and multi collector-inductively coupled plasma-mass spectrometry using standard techniques (see the Appendix for full method details and Table A-1

presenting values of Nd standards run with the dust samples).

We compared Sr and Nd isotope compositions of the dust with two compilations for surficial sediments in potential dust source areas. First, we sampled modern dune systems (n = 12) in western Utah (Fig. A-4). The sites were distributed across ~20,000 km^2 in the Sevier Desert and Great Salt Lake Desert, which are remnants of Pleistocene Lake Bonneville. The samples represent a spectrum from carbonate- and gypsum-dominated sediments to those dominated by silicate minerals. At all sites, approximately 500 g of representative material were collected from the uppermost sediment available for deflation. All were sieved to < 75 μm, and lightly treated with 0.5 M acetic acid before analysis. Ratios of Sr and Nd isotopes in these samples were analyzed at Nanjing University, along with a general geochemical characterization by X-ray fluorescence (see the Appendix for details). Second, we utilized a published compilation presenting 28 potential dust source areas representing a variety of substrates and materials (Fig. A-5) spanning 13° of latitude and 15° of longitude in the western US (Aarons et al., 2017). Samples in this study were collected from the upper 5 cm of surficial material, and were separated into three size fractions (0.2–10 μm, 10–30 μm, and 30–63 μm) before analysis of Sr and Nd isotopes.

3. Results

Grain size analysis reveals that dust accumulating in the alpine zone of the Uinta Mountains has a median grain size of ~10 μm (Fig. 1C). This dominance of fine silt-sized material is consistent from site to site, and from year to year (Munroe, 2014; Munroe et al., 2015). Only ~8% of Uinta dust, by volume, is finer than 2 μm. Comparing with the size classes analyzed by Aarons et al. (2017), ~50% of this material is between 0.2 and 10 μm, ~38% between 10 and 30 μm, and ~10% between 30 and 63 μm.

Ratios of $^{87}Sr/^{86}Sr$ in Uinta dust samples range from 0.71185 to 0.74171, with a mean of 0.71757 (Table 1). Within this range, nearly all the ratios are < 0.73, with a strong clustering between 0.71 and 0.72 (Fig. 2). Two samples, both from the "North" active sampler, are clear outliers, with ratios of ~0.74. Values of ε_{Nd} exhibit a similar pattern, with an overall range from −9.1 to −15.0, a strong clustering between −10 and −11, a mean of −11.3, and nearly all values > −13. The exceptions, once again, are two North samples with values of ~ −15 (Fig. 2).

Plotting the results from the passive samplers (n = 24) in $^{87}Sr/^{86}Sr$ and ε_{Nd} space reveals two distinct clusters of datapoints. The majority of the samples (n = 18, 75%) plot in a focused domain centered on $^{87}Sr/^{86}Sr$ of 0.715 and ε_{Nd} of −10 (Fig. 3A). In contrast, six samples have more radiogenic $^{87}Sr/^{86}Sr$ ratios (0.72 or higher) and slightly more negative ε_{Nd}. All of these samples are winter dust from collectors Dust-1 and Dust-4.

A plausible interpretation of these outliers is revealed by plotting all of the dust results (from both passive and active samplers) along with values for the samples of bedrock measured in this study and other values presented in the literature (Fig. 3B). The thick sequence of siliciclastic rocks comprising the Uinta Mountain Group exhibits considerable stratigraphic, sedimentological, and lithological complexity. Thus, it is not surprising that measured $^{87}Sr/^{86}Sr$ and ε_{Nd} for Uinta bedrock vary widely, and that not all four of the samples measured in this project overlap with previously published results. Nonetheless, it is clear that the Uinta dust samples and bedrock samples are distinct, confirming that the material accumulating in the dust samplers is exotic to the Uinta region. Moreover, the winter samples at Dust-1 and Dust-4, along with the North samples from the active sampler co-located with Dust-1, fall along a mixing line between the dust and rock end members (Fig. 3B). In contrast, summer dust from the active sampler is indistinguishable from summer dust accumulating in the passive samplers. Some collections of dust from the North sampler also exhibit a secondary mode of coarser material (~50 μm, coarse silt) in their grain size distribution (not shown). Together, this evidence suggests that winter dust samples at Dust-1 and Dust-4, as well as the North dust samples, are contaminated by local material.

The contamination of these samples can be explained by the locations of collectors Dust-1 and Dust-4, both of which are positioned relatively close (< 200 m) to north-facing exposures featuring abundant loose regolith and sparsely vegetated soil. Available climatological data indicate that winter winds at high elevations in the Uintas are overwhelmingly from the northwest (Fig. A-2). As these winds sweep up the face of these exposures, they could entrain and transport coarser mineral material to the downwind collectors. Thus, collectors Dust-1 and Dust-4, as well as the north-facing component of the active sampler, likely accumulate a mixture of exotic and local material during winter months. Using the bedrock sample at Dust-1 and the average South dust as end members, a simple mixing model reveals that the North sample contains 60–80% local material, based on $^{87}Sr/^{86}Sr$ and ε_{Nd} respectively, whereas the average winter dust from the Dust-1 passive sampler contains ~20% local material. Due to the asymmetry of the Uinta uplift, similar steep slopes are not present to the south of these collectors. Therefore, accumulation of local material is not an issue in the South dust, or during summer months when prevailing winds are from the south.

Given this interpretation, winter samples from Dust-1 and Dust-4, along with the North samples from the active sampler, are excluded from further discussion of dust in the Uinta alpine zone. The remaining samples (n = 20) of "exotic" dust cluster tightly around a mean $^{87}Sr/^{86}Sr$ ratio of 0.71435 ± 0.00124, and an ε_{Nd} value of −10.5 ± 0.5 (outlined with red oval in Fig. 3A). This composition resembles dust ($^{87}Sr/^{86}Sr$ ~ 0.715, ε_{Nd} ~ −10.5) from the San Juan Mountains of Colorado (Ballantyne et al., 2011; Lawrence et al., 2011; Neff et al., 2008). In contrast, modern dust in the Wind River Range of Wyoming exhibits less radiogenic ε_{Nd} (~ −15) values and similar $^{87}Sr/^{86}Sr$ (0.713) ratios (Brahney et al., 2014).

Ratios of $^{87}Sr/^{86}Sr$ in the Utah dune samples average 0.71186 ± 0.00172, with a maximum of 0.71455 and a minimum of 0.70925 (Table 2). Values of ε_{Nd} average −11.03 ± 0.96, with a maximum of −9.70 and a minimum of −13.33 (Table 2). There is no consistent relationship between $^{87}Sr/^{86}Sr$ or ε_{Nd} and the abundance of CaO or SiO_2. Values of $^{87}Sr/^{86}Sr$ from the dune sediments are also similar to those for carbonate minerals and gypsum from adjacent playas (Carling, unpublished data), indicating that the pre-treatment with dilute acetic acid did not impact the bulk $^{87}Sr/^{86}Sr$ ratios of dune sediments. The pre-treatment likely removed a portion of the calcite but none of the dolomite or gypsum. The remaining portion of these high-Sr minerals would have dominated the $^{87}Sr/^{86}Sr$ ratio of the samples compared with minor amounts of Sr in silicate minerals. Thus, isotopic ratios of dune samples are directly comparable to the Uinta dust samples.

4. Discussion

4.1. Insight into dust source areas

Given the significance of dust deposition to alpine ecosystems in the Rocky Mountains (e.g. Brahney et al., 2014; Lawrence et al., 2013; Painter et al., 2010), and the likelihood that this dust system will evolve with future climate warming, development, and land disturbance (Neff et al., 2008; Reheis and Urban, 2011), it is important to refine our understanding of where this dust is transported from. The measurements of $^{87}Sr/^{86}Sr$ and ε_{Nd} made on Uinta dust samples can provide guidance regarding dust sources. The basic approach of matching fingerprints between dust and surficial materials in possible source areas forms the foundation of dust provenance studies (Grousset and Biscaye, 2005). Challenges with this approach include the likelihood that dust represents a mixture of material from multiple starting locations (Grousset and Biscaye, 2005), the possibility that sorting during transport can impact the isotopic composition of the deposited dust

Table 1
Radiogenic isotope results for Uinta Mountain dust.

Lab Number	Sample ID	Dust-x*	Collection	Season	Analytical Method	Rb ppm	Sr ppm	$^{87}Sr/^{86}Sr$	2-s	Sm ppm	Nd ppm	$^{143}Nd/^{144}Nd$	2-s	$e^{143}Nd$	2-s	Exotic
7Sr-31	JSM-17-18	1	Jul 2012	winter	2017	113.0	163	0.720274	0.000013	–	–	0.512040	0.000006	−11.59	0.12	–
7Sr-30	JSM-17-17	1	Jul 2017	winter	2017	111.4	199	0.718356	0.000010	5.1	26.4	0.511990	0.000007	−12.56	0.14	–
7Sr-14	JSM-17-1	1	Aug 2016	winter	2017	114.2	164	0.725553	0.000012	5.0	12.3	0.512002	0.000007	−12.34	0.14	–
7Sr-15	JSM-17-2	2	Aug 2016	winter	2017	114.4	196	0.714973	0.000011	5.7	13.6	0.512072	0.000007	−10.96	0.14	X
7Sr-16	JSM-17-3	3	Aug 2016	winter	2017	114.7	290	0.713311	0.000011	6.1	13.9	0.512094	0.000007	−10.53	0.14	X
7Sr-17	JSM-17-4	4	Aug 2016	winter	2017	116.0	208	0.721852	0.000014	5.9	14.1	0.511915	0.000007	−14.03	0.14	–
7Sr-18	JSM-17-5	5	Aug 2016	winter	2017	113.1	198	0.716023	0.000010	6.7	15.8	0.512068	0.000007	−11.04	0.14	X
7Sr-19	JSM-17-6	7	Aug 2016	winter	2017	104.7	214	0.714800	0.000011	8.1	18.8	0.512063	0.000007	−11.13	0.14	X
7Sr-20	JSM-17-7	8	Aug 2016	winter	2017	80.9	233	0.712999	0.000009	5.7	13.4	0.512170	0.000007	−9.05	0.14	X
7Sr-21	JSM-17-8	N	Aug 2016	winter	2017	–	–	0.737994	0.000012	–	–	0.511884	0.000009	−14.63	0.18	–
7Sr-22	JSM-17-9	S	Aug 2016	winter	2017	–	–	0.716992	0.000011	–	–	0.512126	0.000008	−9.92	0.16	X
7Sr-23	JSM-17-10	1	Oct 2016	summer	2017	111.8	215	0.715108	0.000011	6.3	15.1	0.512077	0.000008	−10.86	0.16	X
7Sr-24	JSM-17-11	2	Oct 2016	summer	2017	116.8	217	0.713643	0.000013	6.6	15.3	0.512120	0.000007	−10.02	0.14	X
7Sr-25	JSM-17-12	3	Oct 2016	summer	2017	116.3	238	0.713303	0.000011	5.9	13.9	0.512099	0.000007	−10.44	0.14	X
7Sr-26	JSM-17-13	5	Oct 2016	summer	2017	114.6	226	0.713992	0.000011	6.1	14.7	0.512090	0.000006	−10.61	0.12	X
7Sr-27	JSM-17-14	6	Oct 2016	summer	2017	120.9	251	0.713978	0.000011	6.5	14.5	0.512091	0.000007	−10.58	0.14	X
7Sr-28	JSM-17-15	7	Oct 2016	summer	2017	117.2	238	0.714594	0.000009	6.4	14.2	0.512085	0.000007	−10.71	0.14	X
7Sr-29	JSM-17-16	8	Oct 2016	summer	2017	115.8	220	0.714657	0.000010	5.9	13.4	0.512101	0.000008	−10.39	0.16	X
8SR-21	MIDD-18-1	1	Jun 2017	winter	2018	119.4	193	0.720468	0.000010	6.2	14.0	0.512039	0.000014	−11.60	0.28	–
8SR-22	MIDD-18-2	2	Jun 2017	winter	2018	115.4	231	0.713289	0.000009	6.3	13.9	0.512100	0.000007	−10.41	0.13	X
8SR-23	MIDD-18-3	3	Jun 2017	winter	2018	117.2	237	0.712614	0.000011	5.8	13.1	0.512094	0.000008	−10.53	0.16	X
8SR-24	MIDD-18-4	4	Jun 2017	winter	2018	122.9	207	0.718859	0.000009	6.1	14.1	0.511993	0.000005	−12.50	0.09	–
8SR-25	MIDD-18-5	5	Jun 2017	winter	2018	109.8	200	0.715052	0.000010	5.9	13.5	0.512090	0.000013	−10.62	0.26	X
8SR-26	MIDD-18-6	6	Jun 2017	winter	2018	124.9	250	0.711850	0.000010	6.5	15.1	0.512111	0.000007	−10.20	0.14	X
8SR-27	MIDD-18-7	7	Jun 2017	winter	2018	119.2	222	0.715543	0.000010	5.8	13.8	0.512076	0.000002	−10.88	0.04	X
8SR-28	MIDD-18-8	8	Jun 2017	winter	2018	109.3	222	0.715257	0.000011	5.0	11.9	0.512075	0.000009	−10.90	0.17	X
8SR-29	MIDD-18-9	N	Jun 2017	winter	2018	–	–	0.741707	0.000013	–	–	0.511863	0.000017	−15.04	0.32	–
8SR-30	MIDD-18-10	S	Jun 2017	winter	2018	–	–	0.714990	0.000010	–	–	0.512106	0.000014	−10.30	0.27	X
Rock-1	MIDD-18-11	–	–	–	2018	12.5	32.3	0.745561	0.000009	–	–	0.511698	0.000000	−18.26	0.00	–
Rock-2	MIDD-18-12	–	–	–	2018	23.8	66.2	0.726040	0.000010	–	–	0.511731	0.000027	−17.61	0.54	–
Rock-4	MIDD-18-13	–	–	–	2018	22.1	40.5	0.773635	0.000011	–	–	0.511427	0.000021	−23.54	0.40	–
Rock-8	MIDD-18-14	–	–	–	2018	–	–	0.733963	0.000012	–	–	0.511755	0.000002	−17.14	0.04	–

* "x" denotes dust collector number, 1–8. "N" = north active sampler, "S" = south active sampler.

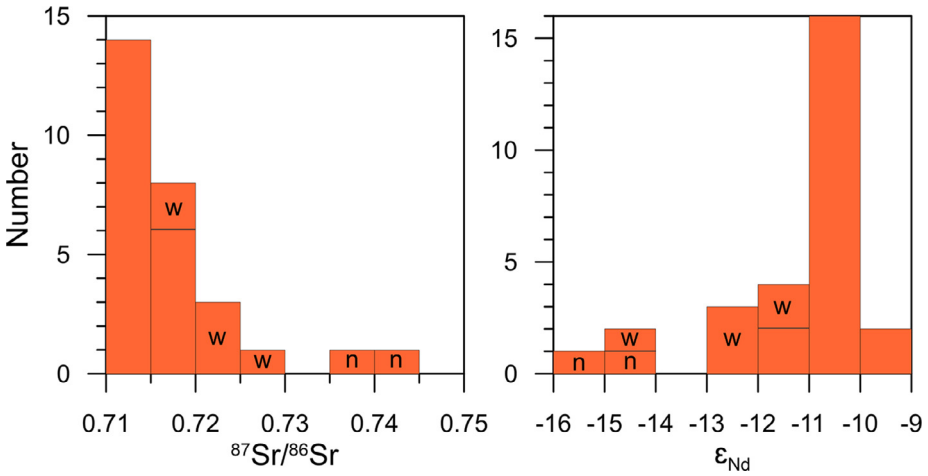

Fig. 2. Histograms of measured $^{87}Sr/^{86}Sr$ ratios and ε_{Nd} values in Uinta dust samples. Results outside the main cluster marked with "n" are from the North active sampler, whereas those marked with "w" are winter samples from Dust-1 and Dust-4.

through density related settling (Aarons et al., 2013), and the obvious impracticality of sampling all possible source areas. Nonetheless, with these caveats in mind, the distribution of measured $^{87}Sr/^{86}Sr$ and ε_{Nd} in modern Uinta dust can be compared with possible source areas to identify locations with a similar isotopic fingerprint. For the purpose of this analysis, a possible source area that plots within the ellipse (within error) delineating exotic Uinta dust (Fig. 3) is considered a match. It is possible that locations plotting outside this ellipse contribute dust to the Uintas, however that dust would need to be mixed with material of another composition to match values seen in the modern Uinta dust.

Given this approach to matching isotopic fingerprints, it is clear that modern dust in the Uinta alpine zone has values of $^{87}Sr/^{86}Sr$ and ε_{Nd} that overlap several of the dune systems sampled in western Utah (Fig. 3C, Table 2). Generally, sites farther from the Uintas exhibit less similarity with Uinta dust (Figs. 4 and A-4); all sites within 250 km of Uintas have a matching isotopic fingerprint, whereas only 1 of the 6 more distant sites matches. The exception, a sample from the Fillmore Dunes ~275 km southwest of the Uintas, is notable because a major fire near this location in 2007 formed an extensive bare area that has been documented as an important dust source (Hahnenberger and Nicoll, 2012; Miller et al., 2012).

Several other sites in the southwestern US also exhibit Sr and Nd isotope compositions similar to the material accumulating in the Uinta alpine zone (Figs. 3C and 4). Prominent among these are locations on the Colorado Plateau in southern Utah, northwestern New Mexico and northern Arizona, as well as three sites in southern Nevada. There is no consistent pattern to the geology of these sites (Fig. A-5), which include both intrusive and extrusive igneous rocks, as well as clastic sedimentary rocks and carbonates (Aarons et al., 2017). At half of these sites, the sampled surficial sediment was alluvium (Fig. A-5), however dunes, playas and other landforms were also sampled (Aarons et al., 2017).

Furthermore, the grain size fraction analyzed does not appear to exert a control over whether the isotopic fingerprint of a site matches Uinta dust (Fig. 4). Seven sites in the finest fraction (0.2–10 μm) analyzed by Aarons et al. (2017) match Uinta dust for both $^{87}Sr/^{86}Sr$ and ε_{Nd}, and 3 additional sites match for just $^{87}Sr/^{86}Sr$ out of a total of 27. The same number, although for a different array of sites, matches in the 10–30 μm size fraction (out of a total of 30). Five sites in the 30–63 μm fraction match Uinta dust for both $^{87}Sr/^{86}Sr$ and ε_{Nd}, 2 additional sites match for $^{87}Sr/^{86}Sr$, and one more for ε_{Nd} Nd (out of 29). Dunes at Coyote Springs (site CS-061414) in southern Nevada are the only locality to match Uinta dust in all three grain size fractions. This result is consistent with the interpretation of Aarons et al. (2017) that weathering to produce successively smaller particles does not result in a more radiogenic $^{87}Sr/^{86}Sr$ ratio.

In contrast, many samples from western Nevada, Colorado, New Mexico, and most samples from southern California are distinct from Uinta dust. A notable spatial cluster of sites that fail to match is located in southwestern Nevada (Fig. 4). Ratios of $^{87}Sr/^{86}Sr$ from these locations are generally < 0.710, and ε_{Nd} is higher than in Uinta dust (> −7). Although the surficial sediment samples in the existing compilation (Aarons et al., 2017) are not evenly distributed in the western US, this pattern nonetheless suggest that some areas, for instance southwestern Nevada, do not function as sources of dust reaching the Uinta Mountains.

The dust sampling strategy employed here inevitably merges multiple dust delivery events, and it is unlikely that any one site would consistently yield dust for transport to the Uintas over the months integrated by these seasonal samples. Thus, Uinta dust is almost certainly a mixture of material derived from multiple sources, which likely explains the range of $^{87}Sr/^{86}Sr$ and ε_{Nd} values for the analyzed samples (Fig. 3). On the other hand, the average fingerprint of all samples in the two compilations used in this study ($^{87}Sr/^{86}Sr$ of 0.71178 and ε_{Nd} of −10.9) is notably distinct from the average Uinta dust. Thus, even if all sites sampled in the western US contribute dust to the Uintas, some must be more significant than others to produce a weighted average that matches Uinta dust. Furthermore, modern Uinta dust has relatively radiogenic $^{87}Sr/^{86}Sr$ in comparison with the sites presented in Aarons et al. (2017). This compilation doesn't represent all possible dust sources in the western US, but it still covers a wide geographic range and array of material and substrates (Fig. A-5), reducing the likelihood that important dust sources with more radiogenic $^{87}Sr/^{86}Sr$ ratios remain unsampled. Either way, the strong correspondence between the radiogenic isotope compositions of the Uinta dust and numerous site compiled in Fig. 4 is confirmation for the theory that arid lands in the southwestern US are responsible for much of the dust arriving at high elevations in the Rocky Mountains.

Relatively few locations to the north and the west of the Uintas are presented in the published compilation (Aarons et al., 2017), and all three sites in Washington and Oregon fail to match Uinta dust (Fig. 4). However, one site on the Snake River Plain of southern Idaho (site SRP-060514), does exhibit a Sr and Nd isotope composition in both the 0.2–10 μm and 30–63 μm fractions similar to Uinta dust (Fig. 4). Furthermore, the radiogenic isotopes at this site match winter dust samples better than summer samples. This result suggests that material deflated from the Snake River Plain is transported to the Uintas in the winter, when prevailing winds are from the northwest (Fig. A-2).

The extensive area of exposed Eocene-age lacustrine sediments in the Green River Basin would also seem a likely dust source given its sparse vegetation and location immediately north of the Uintas.

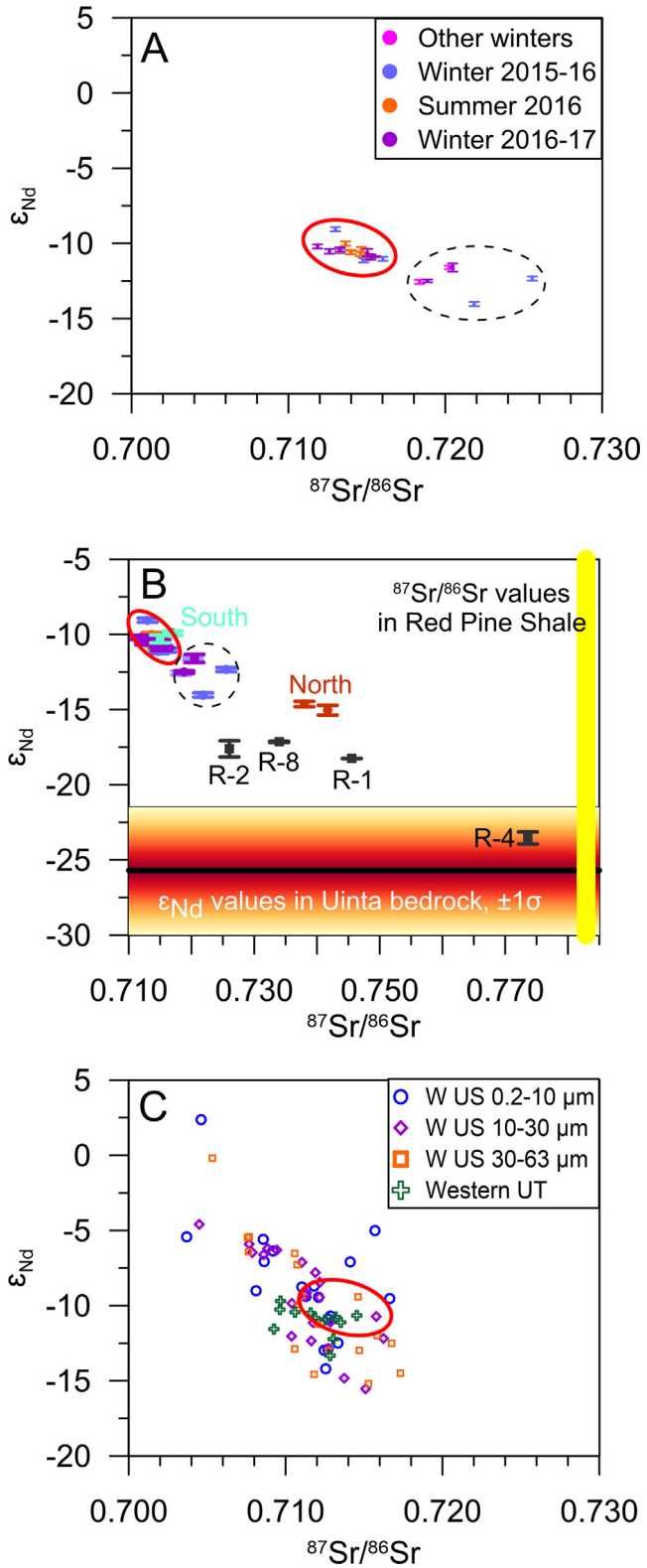

Fig. 3. Isotope results for Uinta Mountain dust and comparison with possible source areas. (A) $^{87}Sr/^{86}Sr$ ratios and ε_{Nd} values in Uinta dust samples from the passive collectors. The dashed ellipse outlines winter samples from Dust-1 and Dust-4 that are contaminated with local material. Red ellipse surrounds exotic dust. 2-σ errors on $^{87}Sr/^{86}Sr$ measurements are smaller than the symbols. (B) Dust results from Fig. 3A plotted with Uinta Mountain bedrock and North and South samples from the active sampler. Black samples denoted by "R-x" are measurements of representative bedrock from the locations of dust collectors 1, 2, 4, and 8. The range of reported ε_{Nd} values in Uinta bedrock (Ball and Farmer, 1998; Condie et al., 2001), as well as an average $^{87}Sr/^{86}Sr$ ratio for the Red Pine Shale at the stratigraphic top of the Uinta Mountain Group bedrock sequence (Crittenden and Peterman, 1975) are also shown. (C) Red ellipse delineating exotic dust in the Uintas (as in Fig. 3A) plotted with $^{87}Sr/^{86}Sr$ ratios and ε_{Nd} values for potential source areas in western Utah (this study), and sites in the western US (W US) (Aarons et al., 2017), divided into 3 grain size fractions.

Although published ratios of $^{87}Sr/^{86}Sr$ for these sediments (~0.710–0.715) are similar to the dust results (Doebbert et al., 2014), values of ε_{Nd} are not available for these sediments. On the other hand, one sample (GRB-060514) (Aarons et al., 2017), collected from alluvium along the Green River, has a $^{87}Sr/^{86}Sr$ ratio similar to Uinta dust (0.7127), but a less radiogenic ε_{Nd} in all size classes (~ −13). Thus if sediments deflated from the Green River Basin form part of the Uinta dust flux, they must be mixed with material with a higher ε_{Nd}.

4.2. Seasonal timing of dust deposition

It is notable that the Sr and Nd isotopes in samples of exotic dust from the passive collectors exhibit such strong consistency between summer and winter seasons (Fig. 3A), because climatic data from the Dust-1 site clearly demonstrate that winds from the south dominate in the summer, whereas northwest winds are more common in the winter (Fig. A-2). However, south winds are also common in April and May (Fig. A-2), two months that are inevitably included in the winter sample (collected in early summer). Thus, at least some of the winter sample is likely delivered by the same southerly winds that bring much of the summer dust. This explanation is supported by reports of greater dust emissions from the southwestern US (Flagg et al., 2014), a greater occurrence of dust storms (Hahnenberger and Nicoll, 2012), and higher concentrations of suspended particulate in the air (Reynolds et al., 2016) during spring months.

Moreover, the masses of winter (~8 months) and summer (~4 months) samples are equivalent despite their contrasting durations (Fig. A-6). This situation is not a result of snow impeding the passive collectors, because the rate of dust accumulation increases with duration of snow cover (Fig. A-7). Instead, the similar mass of the summer sample indicates that southerly winds are dustier. This interpretation is consistent with reports of higher rates of dust deposition in southeastern Utah during the summer (Reheis and Urban, 2011).

Most studies of dust in the Rocky Mountains have focused on dust deposited in winter, which has important consequences for the timing of snow melt (Painter et al., 2010). However, the results reported here indicate that dust deposition during the shorter alpine summer delivers an equivalent mass flux to the alpine zone. This insight enhances other studies that have investigated the role of dust deposition in alpine soil formation and biogeochemical cycling (Aciego et al., 2017; Lawrence et al., 2013, 2011).

4.3. Management implications

The interior regions of the western US shown here to be sources for dust arriving in the Uinta Mountains are vulnerable to a variety of pressures that might increase the entrainment of fine-grained material in the future. Much of the southwestern US, for instance, has been impacted by drought in the early part of the 21st Century (MacDonald, 2010). In addition to straining water supplies for cities and for agriculture, this sustained stretch of drought conditions has lowered water levels in reservoirs and terminal lakes (Wang et al., 2018; Wurtsbaugh et al., 2017), and increased the frequency of wildfires (Dennison et al., 2014); both of these changes enhance the availability of fine surficial materials for wind deflation. Furthermore, numerical models indicate that future droughts are likely to be even more severe (Cayan et al.,

Table 2
$^{87}Sr/^{86}Sr$ and $\varepsilon_{Nd}(0)$ for surficial sediment samples from western Utah.

Site	Number	Latitude (°)	Longitude (°)	$^{87}Sr/^{86}Sr$	$\varepsilon_{Nd}(0)$	Al_2O_3 (%)	BaO (%)	CaO (%)	Cr_2O_3 (%)	Fe_2O_3 (%)	K_2O (%)	MgO (%)	MnO (%)	Na_2O (%)	P_2O_5 (%)	SiO_2 (%)	SrO (%)	TiO_2 (%)	LOI @ 1000° (%)	Total (%)	SO_3 (%)
Tule Valley Dunes	12,469	39.34	−113.44	0.712845	−13.33	0.89	0.07	38.1	< 0.01	0.39	0.24	0.95	0.01	0.09	0.05	4.97	0.24	0.03	11.94	57.97	> 30
Fish Springs Playa Dunes	12,470	39.81	−113.29	0.713041	−12.21	8.70	0.10	13.70	< 0.01	1.13	3.11	1.38	0.03	2.08	0.04	57.62	0.09	0.12	11.75	99.85	–
Fumarole Butte Playa Ripples	12,471	39.57	−112.76	0.711601	−10.50	5.91	0.04	24.5	< 0.01	2.05	1.36	4.31	0.04	2.94	0.10	24.82	0.10	0.25	23.77	90.19	13.45
Sevier Dry Lake Dunes	12,472	39.13	−112.88	0.709252	−11.55	5.26	0.05	6.30	< 0.01	1.25	1.15	1.34	0.03	0.96	0.06	77.83	0.04	0.18	5.14	99.59	–
Knolls Dunes	12,473	40.70	−113.29	0.713176	−10.76	2.27	0.04	36.0	< 0.01	0.61	0.50	1.13	0.01	0.50	0.04	23.46	0.27	0.06	25.35	90.24	10.75
Great Salt Lake Desert Dunes	12,474	40.40	−113.09	0.713530	−11.13	6.96	0.06	6.22	< 0.01	1.80	1.60	1.24	0.03	1.29	0.07	74.79	0.05	0.28	5.00	99.39	–
GSL Dunes at Stansbury Island	12,475	40.77	−112.52	0.714547	−10.67	1.35	0.03	43.1	< 0.01	0.51	0.36	1.98	0.02	0.43	0.13	13.74	0.35	0.06	37.41	99.47	–
Tabernacle Hill Dunes	12,476	38.94	−112.54	0.709678	−9.70	9.06	0.05	2.35	< 0.01	1.57	2.53	0.77	0.03	1.74	0.12	79.72	0.03	0.23	1.92	100.12	–
Little Sahara Dunes	12,477	39.65	−112.31	0.711866	−10.83	6.22	0.04	5.88	0.01	2.22	1.35	1.66	0.04	1.04	0.08	75.71	0.03	0.30	5.09	99.67	–
Fillmore Dunes	12,478	38.92	−112.50	0.712545	−10.93	0.09	0.01	39.1	< 0.01	0.05	0.04	0.28	< 0.01	< 0.01	0.03	1.12	0.23	< 0.01	8.79	49.74	> 30
Holden Dunes	12,479	39.13	−112.41	0.709642	−10.27	7.55	0.04	4.76	0.01	2.23	1.69	1.46	0.03	1.50	0.08	76.53	0.04	0.31	3.35	99.58	–
Oak City Dunes	12,480	39.38	−112.39	0.710600	−10.42	7.20	0.04	5.20	< 0.01	2.37	1.56	1.64	0.04	1.32	0.09	75.19	0.03	0.30	4.28	99.26	–

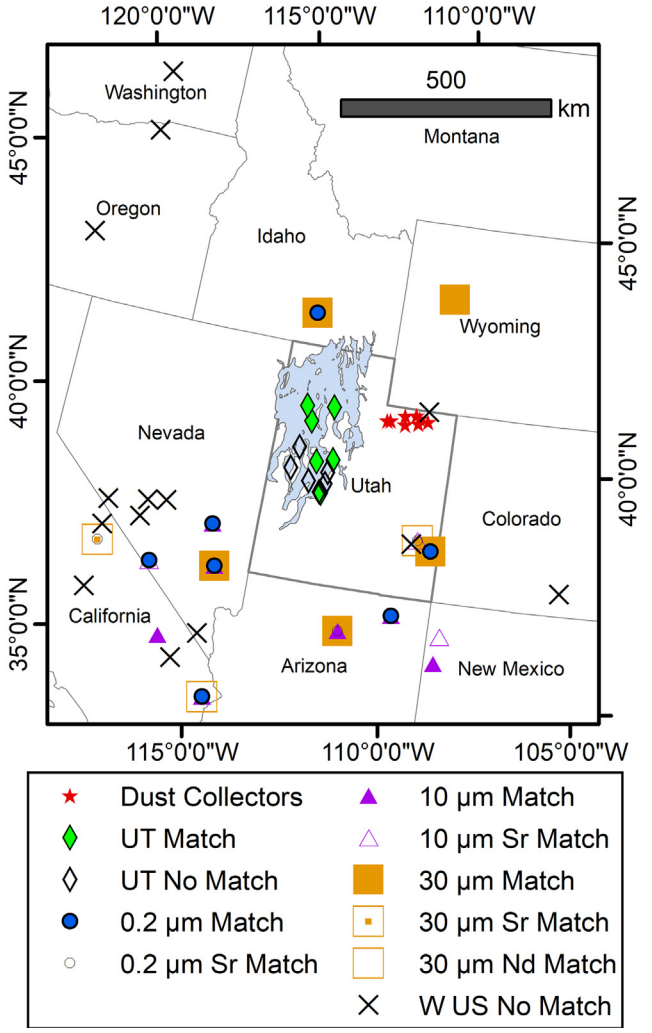

Fig. 4. Potential source areas for Uinta dust in the western United States. Samples in western Utah are from this study (denoted as UT). Data in three grain size fractions (0.2–10 µm, 10–30 µm, and 30–63 µm) are from the western US (W US) compilation (Aarons et al., 2017). Samples denoted as "Sr Match" or "Nd Match" were only analyzed for Sr or Nd respectively. "No Match" denotes a sampling site that does not match the Uinta dust. Red stars mark the dust collectors in the Uinta Mountains. The blue shape denotes pluvial Lake Bonneville at its late Pleistocene highstand. An enlargement focused on the western Utah samples is presented in Fig. A-4.

2010; Cook et al., 2015), making it likely that the emission of dust from this region will further increase. Much land in this region is managed by federal entities such as the Bureau of Land Management, the US Forest Service, and the National Park Service. These agencies work with management plans that are crafted through lengthy processes, and are intended to serve as guiding documents for years or decades after they are written (Forbis et al., 2006). Livestock grazing, mining, clearing for agriculture, oil and gas development, and off-road vehicle use are all examples of regulated activities on federal land with potentially serious implications for persistence of the cryptobiotic crusts that typically stabilize soils in this region (Belnap, 1995; Belnap and Gillette, 1998). Identification of significant dust sources now provides the opportunity, therefore, to inform management plans that will guide important decisions for years in the future.

5. Summary

Using measurements of $^{87}Sr/^{86}Sr$ and ε_{Nd} as an isotopic fingerprint, we have demonstrated that modern aeolian dust is an exotic addition to

the alpine ecosystem of the Uinta Range in the Rocky Mountains. Through comparison with isotopic measurements on samples collected from sand dunes in western Utah, as well as a published compilation of isotopic values for surficial sediments across the western US, we have identified possible sources for this aeolian material. Several locations in southern Utah, northern Arizona, and southern Nevada have surficial sediments with similar isotopic fingerprints. Uinta dust also matches a sample from the Snake River Plain of southern Idaho, indicating that dust transport by northwesterly winds is important, particularly in the winter. In contrast with previous work that focused primarily on dust accumulating in winter, our results indicate that an equivalent mass of dust accumulates in the summer, despite the shorter duration of this season in the high mountains. This insight has important ramifications for studies of biogeochemical cycling and soil development in mountain ecosystems. Recognition that certain specific areas in the southwestern US are sources of dust to the Rocky Mountains, particularly during summer months, should be considered in future land management planning efforts.

CRediT authorship contribution statement

Jeffrey S. Munroe: Conceptualization, Data curation, Formal analysis, Funding acquisition, Investigation, Methodology, Project administration, Resources, Supervision, Validation, Visualization, Writing - original draft, Writing - review & editing. **Emmet D. Norris:** Methodology, Investigation. **Gregory T. Carling:** Methodology, Investigation, Project administration. **Brian L. Beard:** Investigation, Data curation, Supervision. **Aaron M. Satkoski:** Investigation, Supervision. **Lianwen Liu:** Investigation.

Acknowledgements

The field assistance of E. Attwood, C. Hale, D. Munroe, S. O'Keefe, N. Stone, and L. Wasson is appreciated. Thanks to the Ashley National Forest for supporting this project. Funding was provided by NSF-EAR-1524476. Dr. P. Costa and an anonymous reviewer provided constructive feedback that was helpful in improving the manuscript.

Appendix A. Supplementary data

Supplementary data to this article can be found online at https://doi.org/10.1016/j.aeolia.2019.03.005.

References

Aarons, S.M., Aciego, S., Gleason, J., 2013. Variable HfSrNd radiogenic isotopic compositions in a Saharan dust storm over the Atlantic: implications for dust flux to oceans, ice sheets and the terrestrial biosphere. Chem. Geol. 349, 18–26.

Aarons, S.M., Aciego, S.M., Gabrielli, P., Delmonte, B., Koornneef, J.M., Uglietti, C., Wegner, A., Blakowski, M.A., Bouman, C., 2016. Ice core record of dust sources in the western United States over the last 300 years. Chem. Geol. 442, 160–173.

Aarons, S.M., Blakowski, M.A., Aciego, S.M., Stevenson, E.I., Sims, K.W., Scott, S.R., Aarons, C., 2017. Geochemical characterization of critical dust source regions in the American West. Geochim. Cosmochim. Acta 215, 141–161.

Aciego, S.M., Riebe, C.S., Hart, S.C., Blakowski, M.A., Carey, C.J., Aarons, S.M., Dove, N.C., Botthoff, J.K., Sims, K.W.W., Aronson, E.L., 2017. Dust outpaces bedrock in nutrient supply to montane forest ecosystems. Nat. Commun. 8, 14800.

Atwood, W.W., 1909. Glaciation of the Uinta and Wasatch Mountains. US Government Printing Office.

Ball, T.T., Farmer, G.L., 1998. Infilling history of a Neoproterozoic intracratonic basin: Nd isotope provenance studies of the Uinta Mountain Group, Western United States. Precambrian Res. 87, 1–18.

Ballantyne, A.P., Brahney, J., Fernandez, D., Lawrence, C.L., Saros, J., Neff, J.C., 2011. Biogeochemical response of alpine lakes to a recent increase in dust deposition in the Southwestern, US. Biogeosciences 8, 2689.

Belnap, J., 1995. Surface disturbances: their role in accelerating desertification. Environ. Monit. Assess. 37, 39–57. https://doi.org/10.1007/BF00546879.

Belnap, J., Gillette, D.A., 1998. Vulnerability of desert biological soil crusts to wind erosion: the influences of crust development, soil texture, and disturbance. J. Arid Environ. 39, 133–142. https://doi.org/10.1006/jare.1998.0388.

Bockheim, J., Koerner, D., 1997. Pedogenesis in alpine ecosystems of the eastern Uinta Mountains, Utah, USA. Arct. Alp. Res. 29, 164–172.

Bockheim, J., Munroe, J., Douglass, D., Koerner, D., 2000. Soil development along an elevational gradient in the southeastern Uinta Mountains, Utah, USA. Catena 39, 169–185.

Bory, A.-M., Biscaye, P.E., Piotrowski, A.M., Steffensen, J.P., 2003. Regional variability of ice core dust composition and provenance in Greenland. Geochem. Geophys. Geosyst. 4.

Bradley, M.D., 1995. In: Timing of the Laramide Rise of the Uinta Mountains, Utah and Colorado. Guidebook – Wyoming Geological Association, pp. 31–44.

Brahney, J., Ballantyne, A., Kociolek, P., Spaulding, S., Otu, M., Porwoll, T., Neff, J., 2014. Dust mediated transfer of phosphorus to alpine lake ecosystems of the Wind River Range, Wyoming, USA. Biogeochemistry 1–20.

Carling, G.T., Fernandez, D.P., Johnson, W.P., 2012. Dust-mediated loading of trace and major elements to Wasatch Mountain snowpack. Sci. Total Environ. 432, 65–77.

Cayan, D.R., Das, T., Pierce, D.W., Barnett, T.P., Tyree, M., Gershunov, A., 2010. Future dryness in the southwest US and the hydrology of the early 21st century drought. Proc. Natl. Acad. Sci. 107, 21271–21276.

Chen, J., Li, G., Yang, J., Rao, W., Lu, H., Balsam, W., Sun, Y., Ji, J., 2007. Nd and Sr isotopic characteristics of Chinese deserts: implications for the provenances of Asian dust. Geochim. Cosmochim. Acta 71, 3904–3914.

Condie, K.C., Lee, D., Farmer, G.L., 2001. Tectonic setting and provenance of the Neoproterozoic Uinta Mountain and Big Cottonwood groups, northern Utah: constraints from geochemistry, Nd isotopes, and detrital modes. Sed. Geol. 141, 443–464.

Cook, B.I., Ault, T.R., Smerdon, J.E., 2015. Unprecedented 21st century drought risk in the American Southwest and Central Plains. Sci. Adv. 1, e1400082.

Crittenden, M.D., Peterman, Z., 1975. Provisional Rb/Sr age of the Precambrian Uinta Mountain Group, northeastern Utah. Utah Geology 2 GeoRef.

Dastrup, D.B., Carling, G.T., Collins, S.A., Nelson, S.T., Fernandez, D.P., Tingey, D.G., Hahnenberger, M., Aanderud, Z.T., 2018. Aeolian dust chemistry and bacterial communities in snow are unique to airshed locations across northern Utah, USA. Atmos. Environ.

Dehler, C.M., Porter, S.M., De Grey, L.D., Sprinkel, D.A., Brehm, A., 2007. The Neoproterozoic Uinta Mountain Group revisited; a synthesis of recent work on the Red Pine Shale and related undivided clastic strata, northeastern Utah, U. S. A. Spec. Publ. Soc. Sediment. Geol. 86, 151–166.

Dennison, P.E., Brewer, S.C., Arnold, J.D., Moritz, M.A., 2014. Large wildfire trends in the western United States, 1984–2011. Geophys. Res. Lett. 41, 2928–2933. https://doi.org/10.1002/2014GL059576.

Doebbert, A.C., Johnson, C.M., Carroll, A.R., Beard, B.L., Pietras, J.T., Carson, M.R., Norsted, B., Throckmorton, L.A., 2014. Controls on Sr isotopic evolution in lacustrine systems: Eocene green river formation, Wyoming. Chem. Geol. 380, 172–189.

Flagg, C.B., Neff, J.C., Reynolds, R.L., Belnap, J., 2014. Spatial and temporal patterns of dust emissions (2004–2012) in semi-arid landscapes, southeastern Utah, USA. Aeolian Res. 15, 31–43. https://doi.org/10.1016/j.aeolia.2013.10.002.

Forbis, T.A., Provencher, L., Frid, L., Medlyn, G., 2006. Great Basin land management planning using ecological modeling. Environ. Manage. 38, 62–83. https://doi.org/10.1007/s00267-005-0089-2.

Goldstein, H.L., Reynolds, R.L., Reheis, M.C., Yount, J.C., Neff, J.C., 2008. Compositional trends in aeolian dust along a transect across the southwestern United States. J. Geophys. Res. Earth Surf. 113.

Goossens, D., Offer, Z.Y., 2000. Wind tunnel and field calibration of six aeolian dust samplers. Atmos. Environ. 34, 1043–1057. https://doi.org/10.1016/S1352-2310(99)00376-3.

Grousset, F.E., Biscaye, P.E., 2005. Tracing dust sources and transport patterns using Sr, Nd and Pb isotopes. Chem. Geol. 222, 149–167. https://doi.org/10.1016/j.chemgeo.2005.05.006.

Hahnenberger, M., Nicoll, K., 2014. Geomorphic and land cover identification of dust sources in the eastern Great Basin of Utah, USA. Geomorphology 204, 657–672.

Hahnenberger, M., Nicoll, K., 2012. Meteorological characteristics of dust storm events in the eastern Great Basin of Utah, USA. Atmos. Environ. 60, 601–612.

Kumar, A., Abouchami, W., Galer, S.J.G., Garrison, V.H., Williams, E., Andreae, M.O., 2014. A radiogenic isotope tracer study of transatlantic dust transport from Africa to the Caribbean. Atmos. Environ. 82, 130–143.

Laabs, B.J.C., Carson, E.C., 2005. Glacial geology of the southern Uinta Mountains. In: Dehler, C.M., Pederson, J.L., Sprinkel, D.A., Kowallis, B.J. (Eds.), Uinta Mountain Geology. Utah Geological Survey, pp. 235–253.

Lawrence, C.R., Neff, J.C., 2009. The contemporary physical and chemical flux of aeolian dust; a synthesis of direct measurements of dust deposition. Chem. Geol. 267, 46–63. https://doi.org/10.1016/j.chemgeo.2009.02.005.

Lawrence, C.R., Neff, J.C., Farmer, G.L., 2011. The accretion of aeolian dust in soils of the San Juan Mountains, Colorado, USA. J. Geophys. Res. 116, F02013. https://doi.org/10.1029/2010JF001899.

Lawrence, C.R., Painter, T.H., Landry, C.C., Neff, J.C., 2010. Contemporary geochemical composition and flux of aeolian dust to the San Juan Mountains, Colorado, United States. J. Geophys. Res. 115, G03007. https://doi.org/10.1029/2009JG001077.

Lawrence, C.R., Reynolds, R.L., Ketterer, M.E., Neff, J.C., 2013. Aeolian controls of soil geochemistry and weathering fluxes in high-elevation ecosystems of the Rocky Mountains, Colorado. Geochim. Cosmochim. Acta 107, 27–46.

Lupker, M., Aciego, S.M., Bourdon, B., Schwander, J., Stocker, T.F., 2010. Isotopic tracing (Sr, Nd, U and Hf) of continental and marine aerosols in an 18th century section of the Dye-3 ice core (Greenland). Earth Planet. Sci. Lett. 295, 277–286.

MacDonald, G.M., 2010. Water, climate change, and sustainability in the southwest. Proc. Natl. Acad. Sci. 107, 21256–21262.

Mahowald, N.M., Baker, A.R., Bergametti, G., Brooks, N., Duce, R.A., Jickells, T.D., Kubilay, N., Prospero, J.M., Tegen, I., 2005. Atmospheric global dust cycle and iron inputs to the ocean. Global Biogeochem. Cycles 19.

Marx, S.K., Kamber, B.S., McGowan, H.A., Petherick, L.M., McTainsh, G.H., Stromsoe, N., Hooper, J.N., May, J.-H., 2018. Palaeo-dust records: a window to understanding past environments. Global Planet. Change 165, 13–43.
Miller, M.E., Bowker, M.A., Reynolds, R.L., Goldstein, H.L., 2012. Post-fire land treatments and wind erosion–lessons from the Milford Flat Fire, UT, USA. Aeolian Res. 7, 29–44.
Munroe, J.S., 2014. Properties of modern dust accumulating in the Uinta Mountains, Utah, USA, and implications for the regional dust system of the Rocky Mountains. Earth Surf. Process. Landforms 39, 1979–1988.
Munroe, J.S., 2007. Properties of alpine soils associated with well-developed sorted polygons in the Uinta Mountains, Utah, USA. Arct. Antarct. Alp. Res. 39, 578–591.
Munroe, J.S., 2006. Investigating the spatial distribution of summit flats in the Uinta Mountains of northeastern Utah, USA. Geomorphology 75, 437–449.
Munroe, J.S., 2005. Glacial geology of the northern Uinta Mountains. In: Dehler, C.M., Pederson, J.L., Sprinkel, D.A., Kowallis, B.J. (Eds.), Uinta Mountain Geology. Utah Geological Survey, pp. 215–234.
Munroe, J.S., Attwood, E.C., O'Keefe, S.S., Quackenbush, P.J., 2015. Eolian deposition in the alpine zone of the Uinta Mountains, Utah, USA. Catena 124, 119–129.
Munroe, J.S., Laabs, B.J.C., 2009. Glacial Geologic Map of the Uinta Mountains Area, Utah and Wyoming. Utah Geological Survey Miscellaneous Publication 09-4DM.
Neff, J.C., Ballantyne, A.P., Farmer, G.L., Mahowald, N.M., Conroy, J.L., Landry, C.C., Overpeck, J.T., Painter, T.H., Lawrence, C.R., Reynolds, R.L., 2008. Increasing eolian dust deposition in the western United States linked to human activity. Nat. Geosci. 1, 189–195. https://doi.org/10.1038/ngeo133.
Painter, T.H., Barrett, A.P., Landry, C.C., Neff, J.C., Cassidy, M.P., Lawrence, C.R., McBride, K.E., Farmer, G.L., 2007. Impact of disturbed desert soils on duration of mountain snow cover. Geophys. Res. Lett. 34, L12502. https://doi.org/10.1029/2007GL030284.
Painter, T.H., Deems, J.S., Belnap, J., Hamlet, A.F., Landry, C.C., Udall, B., 2010. Response of Colorado River runoff to dust radiative forcing in snow. Proc. Natl. Acad. Sci. 107, 17125–17130.
Painter, T.H., Skiles, S.M., Deems, J.S., Brandt, W.T., Dozier, J., 2018. Variation in rising limb of Colorado River snowmelt runoff hydrograph controlled by dust radiative forcing in snow. Geophys. Res. Lett. 45, 797–808.
Painter, T.H., Skiles, S.M., Deems, J.S., Bryant, A.C., Landry, C.C., 2012. Dust radiative forcing in snow of the Upper Colorado River Basin: 1. A 6 year record of energy balance, radiation, and dust concentrations. Water Resour. Res. 48.
Pourmand, A., Prospero, J.M., Sharifi, A., 2014. Geochemical fingerprinting of trans-Atlantic African dust based on radiogenic Sr-Nd-Hf isotopes and rare earth element anomalies. Geology 42, 675–678.
Prospero, J.M., Ginoux, P., Torres, O., Nicholson, S.E., Gill, T.E., 2002. Environmental characterization of global sources of atmospheric soil dust identified with the Nimbus 7 Total Ozone Mapping Spectrometer (TOMS) absorbing aerosol product. Rev. Geophys. 40.
Psenner, R., 1999. Living in a dusty world: airborne dust as a key factor for alpine lakes. Water Air Soil Pollut. 112, 217–227. https://doi.org/10.1023/A:1005082832499.
Reheis, M.C., Kihl, R., 1995. Dust deposition in southern Nevada and California, 1984–1989: relations to climate, source area, and source lithology. J. Geophys. Res. D 100, 8893–8918.
Reheis, M.C., Urban, F.E., 2011. Regional and climatic controls on seasonal dust deposition in the southwestern US. Aeolian Res. 3, 3–21.
Reynolds, R.L., Goldstein, H.L., Moskowitz, B.M., Bryant, A.C., Skiles, S.M., Kokaly, R.F., Flagg, C.B., Yauk, K., Berquó, T., Breit, G., 2013. Composition of dust deposited to snow cover in the Wasatch Range (Utah, USA): controls on radiative properties of snow cover and comparison to some dust-source sediments. Aeolian Res. 15, 73–90.
Reynolds, R.L., Mordecai, J.S., Rosenbaum, J.G., Ketterer, M.E., Walsh, M.K., Moser, K.A., 2010. Compositional changes in sediments of subalpine lakes, Uinta Mountains (Utah): evidence for the effects of human activity on atmospheric dust inputs. J. Paleolimnol. 44, 161–175.
Reynolds, R.L., Munson, S.M., Fernandez, D., Goldstein, H.L., Neff, J.C., 2016. Concentrations of mineral aerosol from desert to plains across the central Rocky Mountains, western United States. Aeolian Res. 23, 21–35.
Sears, J., Graff, P., Holden, G., 1982. Tectonic evolution of lower Proterozoic rocks, Uinta Mountains, Utah and Colorado. Geol. Soc. Am. Bull. 93, 990–997.
Skiles, S.M., Painter, T., 2017. Daily evolution in dust and black carbon content, snow grain size, and snow albedo during snowmelt, Rocky Mountains, Colorado. J. Glaciol. 63, 118–132.
Skiles, S.M., Painter, T.H., Deems, J.S., Bryant, A.C., Landry, C.C., 2012. Dust radiative forcing in snow of the Upper Colorado River Basin: 2. Interannual variability in radiative forcing and snowmelt rates. Water Resour. Res. 48.
Sow, M., Goossens, D., Rajot, J.L., 2006. Calibration of the MDCO dust collector and of four versions of the inverted frisbee dust deposition sampler. Geomorphology 82, 360–375. https://doi.org/10.1016/j.geomorph.2006.05.013.
Újvári, G., Stevens, T., Svensson, A., Klötzli, U.S., Manning, C., Németh, T., Kovács, J., Sweeney, M.R., Gocke, M., Wiesenberg, G.L., 2015. Two possible source regions for central Greenland last glacial dust. Geophys. Res. Lett. 42.
Wang, J., Song, C., Reager, J.T., Yao, F., Famiglietti, J.S., Sheng, Y., MacDonald, G.M., Brun, F., Schmied, H.M., Marston, R.A., Wada, Y., 2018. Recent global decline in endorheic basin water storages. Nat. Geosci. 11, 926. https://doi.org/10.1038/s41561-018-0265-7.
Wang, Y.-X., Yang, J.-D., Chen, J., Zhang, K.-J., Rao, W.-B., 2007. The Sr and Nd isotopic variations of the Chinese Loess Plateau during the past 7 Ma: implications for the East Asian winter monsoon and source areas of loess. Palaeogeogr. Palaeoclimatol. Palaeoecol. 249, 351–361.
Wurtsbaugh, W.A., Miller, C., Null, S.E., DeRose, R.J., Wilcock, P., Hahnenberger, M., Howe, F., Moore, J., 2017. Decline of the world's saline lakes. Nat. Geosci. 10, 816.
Zhang, Z., Goldstein, H.L., Reynolds, R.L., Hu, Y., Wang, X., Zhu, M., 2018. Phosphorus speciation and solubility in aeolian dust deposited in the interior American West. Environ. Sci. Technol. 52, 2658–2667.
Zhao, W., Balsam, W., Williams, E., Long, X., Ji, J., 2018. Sr–Nd–Hf isotopic fingerprinting of transatlantic dust derived from North Africa. Earth Planet. Sci. Lett. 486, 23–31.